

# Gravitational lensing by $k - n$ generalized black-bounce space-times

C. Furtado,<sup>1,\*</sup> A. L. A. Moreira,<sup>1,†</sup> J. R.

Nascimento,<sup>1,‡</sup> A. Yu. Petrov,<sup>1,§</sup> and P. J. Porfírio<sup>1,¶</sup>

<sup>1</sup>*Departamento de Física, Universidade Federal da Paraíba,  
Caixa Postal 5008, 58051-970, João Pessoa, Paraíba, Brazil.*

## Abstract

We study gravitational lensing by  $k - n$  generalized black-bounce space-times both in regimes of weak and strong field approximations. These metrics interpolate between regular black holes and one-way or traversable wormholes. First, we investigate the light-like geodesic trajectories and derive an analytical expression for the deflection angle in terms of the bounce parameter in the weak-field gravitational regime. We then turn to the strong-field gravitational regime and display the behavior of the bending angle as a function of both the impact parameter and the bounce parameter. Next, using the lens equations, we analyze how the observables for *Sagittarius A\** behave concerning the bounce parameter. We obtain the shadow's radii for some black-bounce metrics and plot the graph of their sizes, comparing them with the Schwarzschild one.

---

\*Electronic address: furtado@fisica.ufpb.br

†Electronic address: toinho.alam@gmail.com

‡Electronic address: jroberto@fisica.ufpb.br

§Electronic address: petrov@fisica.ufpb.br

¶Electronic address: pporfirio@fisica.ufpb.br

## I. INTRODUCTION

It is undeniable that general relativity (GR) remains our best-tested theory of gravity. This statement is underpinned by its remarkable success in describing numerous gravitational phenomena, such as classical tests and gravitational waves. One notable gravitational phenomenon is gravitational lensing – the light deflection in the neighborhood of a massive object (often referred to as a gravitational lens). In fact, this effect was originally observed over one hundred years ago [1] (the history of this discovery is presented in various papers, see, for example, [2, 3]). Recent breakthroughs, such as obtaining the image of the shadow of a supermassive black hole at the center of the M87 galaxy [4–9], and, furthermore, the observation of the supermassive black hole *Sagittarius A\** located at the center of our galaxy [10], have further increased interest in the study of gravitational lensing.

Due to mathematical difficulties, the first works regarding gravitational lensing were carried out in the limit when the light passes far from the gravitational lens (given by some massive object) – this approximation is sometimes referred to as the weak gravitational field regime [11–13]. Nevertheless, the weak-field regime fails to apply when light experiences an intense gravitational field; this is known as the strong gravitational field regime. In the latter case, a typical example arises as the light passes near the photon sphere – that is, a region where the gravitational pull is so strong that the circular lightlike geodesics become unstable – of a black hole. In this limit, several works have been performed to compute the angular deflection in different contexts, including quantum gravity inspired black holes [14–16], non-commutative black holes [17–19], Reissner-Nordström black holes [20–22], wormholes [23–36], spinning black holes [37–43]. The keystone of the theoretical studies of strong gravitational lensing has been put forward by the seminal paper [44], where strong gravitational lensing by a Schwarzschild black hole has been studied. The authors found a surprising effect: an infinite sequence of relativistic images, aside from the primary and secondary images, has been generated along the optic axis, which is a purely effect of the strong field regime. Further continuation of this study has been performed in [45] where the concept of photon surface generalizing the photon sphere was proposed. Afterwards, several mathematically consistent approaches to the formal study of gravitational lensing in the strong field regime were developed in [46–49]. Recent results for strong deflection of particles in various contexts are presented in [14, 50–54], and some other issues related to

gravitational lensing can be found also in [55, 56].

It is well known that GR presents pathological solutions, for example, i) the Gödel solution in which global causality is broken, and ii) solutions that display singularities, such as the Schwarzschild black hole. Regarding the latter, Bardeen originally proposed a black hole solution without singularity, the so-called regular black hole [57]. Other regular black hole solutions have been obtained in the literature [58–63]; in particular, we highlight a class of metrics known as black-bounce ones, which describe non-singular solutions [64, 65]. Furthermore, regular black holes have the peculiar property of being sourced by a matter content that violates the energy conditions in GR [66]. Although this is a stringent constraint in GR, it generically does not hold in alternative theories of gravity scenarios. Within the light deflection context, an important study of regular black holes has been carried out in [67], the effect of weak and strong gravitational lensing has been studied in the Simpson-Visser (SV) black-bounce space-time, originally introduced in [64]. In this paper, we do the next step along this line considering a more generic regular metric called  $k - n$  generalized black-bounce space-time [68] which reduces to the one studied in [67] for special values of the parameters. For this metric, we consider the light deflection both for weak-field and strong-field limits.

The structure of the paper is as follows. In Section II, we briefly describe the main properties of generalized black-bounce space-times. In Section III, we consider the light deflection in the weak field regime within these regular space-times and then we compute its correspondent deflection angle. In Section IV, employing Tsukamoto’s method, we plot the graphs of angular deflection in terms of the impact parameter. Section V is devoted to a detailed discussion of gravitational lensing by the generalized black-bounce metrics and to its applications, such as obtaining observables from observational data of *Sagittarius A\** and investigating the sizes of the shadows. We summarize our results in Section VI.

## II. GENERALIZED BLACK-BOUNCE SPACE-TIMES

One of the most interesting studies of the light deflection has been performed in the standard black-bounce space-time [67, 69], also known as the SV space-time, which represents itself as one of the simplest examples of a regular black hole (various issues relating to this solution, including a discussion of corresponding matter sources, can be found in [70]).

Later, various generalizations of this metric have been introduced, see, e.g., [68]. They are characterized by the typical form of the line element:

$$ds^2 = f(r)dt^2 - \frac{dr^2}{f(r)} - \Sigma^2(r)(d\theta^2 + \sin^2\theta d\phi^2), \quad (1)$$

where  $\Sigma(r) = \sqrt{r^2 + a^2}$  and  $f(r) = 1 - \frac{2M(r)}{\Sigma(r)}$  [68]. The dependence on the bounce parameter  $a$ , allowing to avoid the presence of a singularity, is the main feature of all black-bounce space-times. It corresponds to a throat at the origin, which may or may not be surrounded by an event horizon. Depending on the value of  $a$ , the metric (1) can describe a regular black hole with a space-like throat leading into a future copy of the universe, a one-way wormhole if the throat is light-like, or even a traversable wormhole if the throat is time-like. These space-times present mostly the same properties as SV ones, but some of them can have more than one horizon, and some of them can violate only some of the energy conditions required in GR instead of all of them. It is possible that these metrics do not violate the energy conditions in some modified theories of gravitation.

The main difference of the metric (1) from the SV one is the generalization of the constant mass to a function of the radial coordinate  $M(r)$ , which can carry additional parameters and generate new effects. The example of space-time proposed in [68] introduces the parameters  $k$  (a nonnegative integer) and  $n$  (a positive integer) by defining

$$M(r) = \frac{m\Sigma(r)r^k}{(r^{2n} + a^{2n})^{\frac{k+1}{2n}}}. \quad (2)$$

The SV metric corresponds to the case with  $n = 1$  and  $k = 0$ . In any of the new black-bounce space-times,  $a \rightarrow 0$  recovers the Schwarzschild space-time. These metrics have the same restrictions in GR as the SV one, i.e., in general they do not satisfy the energy conditions, requiring some source of exotic matter whose distribution through space is discussed in detail in [68], but they have the advantage that this mass function  $M(r)$  can be modified to avoid violating at least some energy conditions, in a modified theory of gravitation.

Our goal hereby is to calculate the light deflection and consequently gravitational lensing effects in some of the generalized black-bounce space-times. A more specific characterization of some of these metrics will be given in Section IV where we study the photon spheres for the metrics with  $k = 0, n = 2$  and  $k = 2, n = 1$ .

### III. LIGHT DEFLECTION: WEAK FIELD REGIME

The trajectory of the photon moving through the space-times described by the metric (1), with the mass function given by (2) is determined by the Lagrangian

$$\mathcal{L} = \left(1 - \frac{2mr^k}{(r^{2n} + a^{2n})^{\frac{k+1}{2n}}}\right) \dot{t}^2 - \left(1 - \frac{2mr^k}{(r^{2n} + a^{2n})^{\frac{k+1}{2n}}}\right)^{-1} \dot{r}^2 - (r^2 + a^2)(\dot{\theta}^2 + \sin^2 \theta \dot{\phi}^2). \quad (3)$$

For the light-like particle we have the constraint  $\mathcal{L} = 0$ . Using the Euler-Lagrange equation for  $t$ , we obtain the following expression for the photon energy:

$$E = \left(1 - \frac{2mr^k}{(r^{2n} + a^{2n})^{\frac{k+1}{2n}}}\right) \dot{t}. \quad (4)$$

The evident homogeneity of time allows us to conclude the energy of the photon is conserved, which is natural since the metric is static. Further, from the Euler-Lagrange equation for  $\phi$ , we see that the  $z$ -component of angular momentum of the photon, given by

$$L = (r^2 + a^2) \sin^2 \theta \dot{\phi} \quad (5)$$

is also conserved. As a consequence, the trajectory of the photon is restricted to a single equatorial plane, and we can assume  $\theta = \frac{\pi}{2}$ . Taking into account the spherical symmetry of the metric, we can easily find the trajectory of the photon.

If we substitute (4) and (5) in (3), and require  $\theta = \pi/2$ , we get

$$E^2 = \dot{r}^2 + L^2 \left(1 - \frac{2mr^k}{(r^{2n} + a^{2n})^{\frac{k+1}{2n}}}\right) (r^2 + a^2)^{-1} \quad (6)$$

So, the problem of finding the trajectory of light reduces to that of a one-dimensional movement for a particle under the effective potential  $V(r) \equiv L^2 \frac{f(r)}{\Sigma^2(r)}$  displayed at Fig. 1.

Each photon coming from infinity has an impact parameter  $b = \frac{L}{E}$ , which determines its behavior in response to  $V$ , and consequently its trajectory. Depending on its value, the photon can either be scattered in some direction, fall into the black hole, or, in the strong field limit, stay orbiting around it indefinitely in the photon sphere. There is a maximal approximation point ( $r_0$ ) that can be found for every impact parameter. In other words, when a photon comes from infinity, it passes near the black hole at a minimal distance  $r_0$  and is scattered in another direction afterward. The angle between its trajectories before and after scattering is the deflection angle which we will denote as  $\alpha$ .

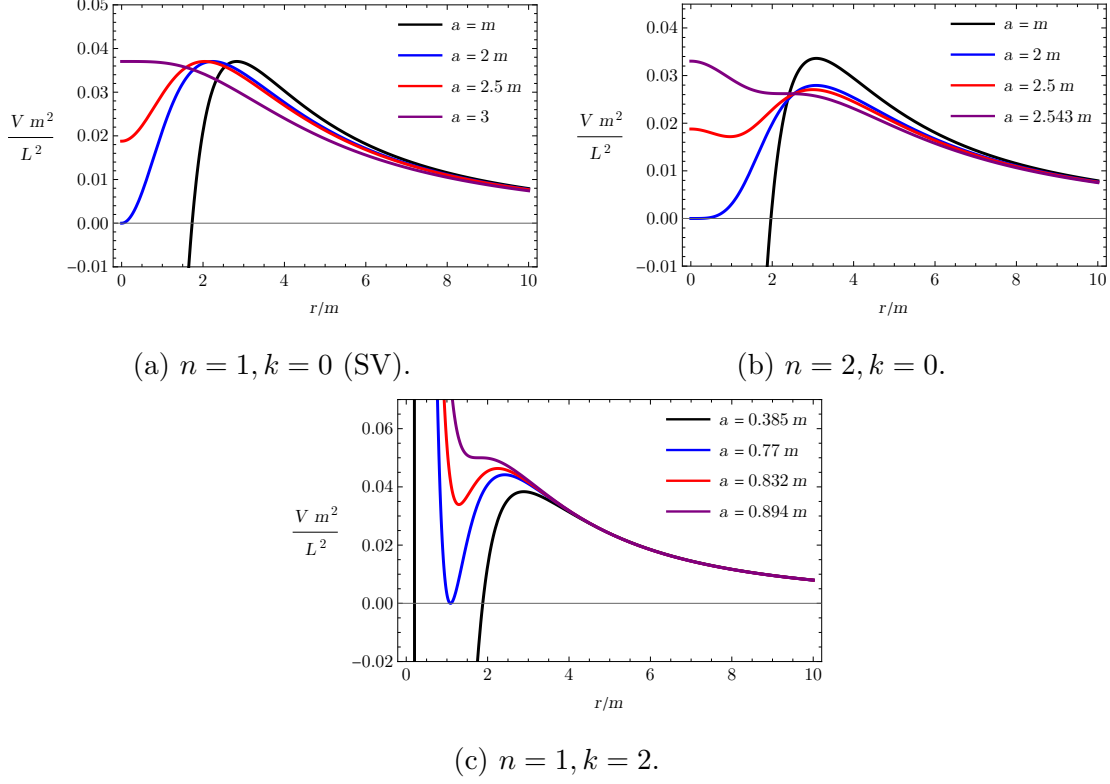


Figure 1: Effective potentials for some specific black-bounce spacetimes.

Since the impact parameter is constant for the entire trajectory, its value is easily obtained by knowing  $r_0$ , because at this point  $\dot{r} = 0$ , and from (6) we have  $b^2 = \frac{\Sigma^2(r_0)}{f(r_0)}$ . Rewriting (6) with use of the definitions of the effective potential  $V$ , the impact parameter  $b$  and the angular momentum  $L$ , we obtain a trajectory equation relating  $r$  and the angular coordinate  $\phi$ :

$$\dot{r}^2 = \dot{\phi}^2 \Sigma^4(r) \left( \frac{1}{b^2} - \frac{f(r)}{\Sigma^2(r)} \right) \quad (7)$$

We can then define  $\alpha$  from this equation by integrating the angle where radius varies from  $r_0$  to  $\infty$  to obtain the first branch of the trajectory, multiplying the result by 2, and then subtracting  $\pi$ , so, finally we obtain

$$\alpha = 2 \int_{r_0}^{\infty} \frac{dr}{\sqrt{\frac{\Sigma^4(r) f(r_0)}{\Sigma(r_0)} - f(r) \Sigma^2(r)}} - \pi. \quad (8)$$

This integral cannot be expressed in closed form, so, it must be approximated in some way. It can be found using some numerical approximation, as in Fig. 2. At the same time, several physically interesting results can be obtained through expansions of this integral. We first consider light deflection in the weak field limit, that is, when  $m \ll 1$ , and consequently

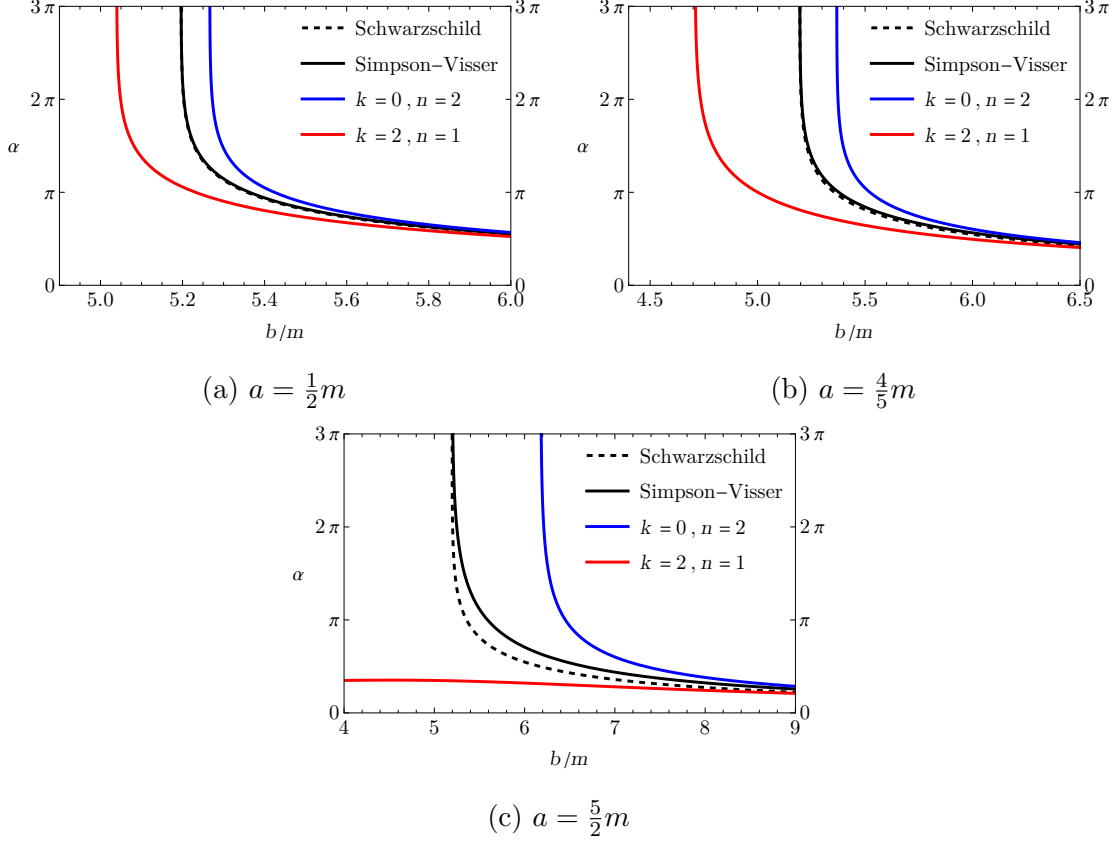


Figure 2: Light deflection as a function of the impact parameter for different space-times with the same value of  $a$ .

$a \ll 1$ . This scenario corresponds to the large distance from the center of the black hole. In the zeroth order, we have zero result which is natural since the black hole should not affect regions very distant from it. In this limit  $r_0 \approx b$ , so we express the result in terms of  $b$ . Then, we can write down the Taylor series up to the second order, to obtain the deflection in every black-bounce space-time:

$$\alpha \approx \frac{4m}{b} + \frac{(15\pi - 16)m^2}{4b^2} + \frac{\pi a^2}{4b^2} \quad (9)$$

as is the case for SV space-time. Therefore we conclude that in the weak field limit the new black-bounce space-times cannot be distinguished from the SV space-time.

#### IV. LIGHT DEFLECTION: STRONG FIELD REGIME

Now we turn to the strong field limit. In this case, we give main attention to the light deflection near the photon sphere, whose radius is  $r_m$ . Since these metrics are spherically

symmetric, static and asymptotically flat, we can use the same procedure developed in [49] to calculate the deflection of light in our case. The first step is to calculate the radius of the photon sphere ( $r_m$ ), for which the following expression is valid:

$$V'(r_m) = 0. \quad (10)$$

In this expression, the prime denotes the derivative with respect to the coordinate  $r$ . This expression itself could describe a maximum or a minimum of the effective potential, but for the metrics studied here, the outermost photon sphere, or the largest solution of (10) is always a maximum. Indeed, if there was a minimum, the photon would have a greater energy than is needed to be caught in the potential well and would pass right through it. Where there is a maximum potential, it becomes an unstable equilibrium point. If the innermost radius attained by the photon ( $r_0$ ) coincides with the photon sphere ( $r_m$ ), the photon becomes trapped in it forever moving around the black hole. In practice, two situations occur, namely: if  $r_0 < r_m$ , the photon follows an unstable circular orbit and then falls inside the black hole, and if  $r_0 > r_m$ , the photon is scattered by the black hole to infinity. As its energy approaches its maximum, it circles the black hole an increasing number of times. This scenario will become more important in Section V. Now we are concerned with the dependence of the deflection angle on the parameters of the metric.

To start, let us consider the case with  $k = 2$  and  $n = 1$  (Fig. 3a) and the case with  $k = 0$  and  $n = 2$  (Fig. 3b). Other space-times with  $n = 1$  and  $k \neq 0, 2$  have configurations of event horizon and photon sphere analogous to 3a. Similarly, other space-times with  $n > 1$  and for all  $k$  behave like 3b. The differences among the different kinds of black-bounce metrics are

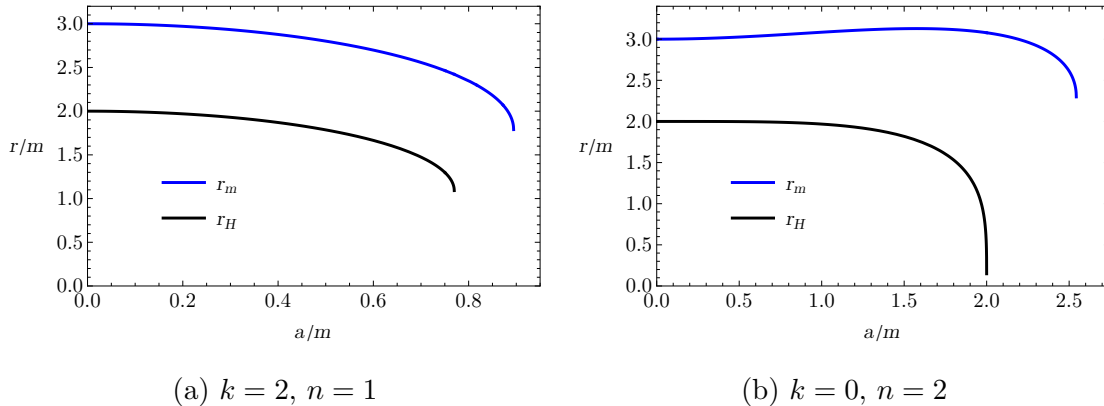


Figure 3: Photon sphere (blue) and event horizon (black) for black-bounce space-times.



more evident as we approach the photon spheres.

Let us now proceed with an in-depth assessment of the horizon and photon sphere structures of some particular black-bounce metrics. To gain more insight on this, we first consider the SV metric, which possesses the following features:

- a horizon at  $r_H = \sqrt{(2m)^2 - a^2}$  and a photon sphere at  $r_m = \sqrt{9m^2 - a^2}$  for  $0 \leq a < 2m$ ;
- a marginal horizon at  $r_H = 0$  and a photon sphere at  $r_m = \sqrt{5}m$  for  $a = 2m$ ;
- no horizon and a photon sphere for  $2m < a < 3m$ ;
- no horizon and a marginal photon sphere at  $r_m = 0$  for  $a = 3m$ ;
- no horizon and no photon sphere for  $a > 3m$ .

Now, let us explore two different cases for the generalized black-bounce metrics, namely:

- for  $n = 2$  and  $k = 0$  and  $a < 2m$ , we found one horizon at  $r_H = \sqrt[4]{(2m)^4 - a^4}$  and one photon sphere whose radius is given by the equation

$$3mr_m^5 + ma^2r_m^3 + 2ma^4r_m = (r_m^5 + a^4r_m)\sqrt[4]{r_m^4 + a^4}, \quad (11)$$

for  $a = 2m$  it has a marginal horizon at  $r_H = 0$  besides one photon sphere, for  $2m < a < 2.54343m$  it has an inner and an outer photon sphere, for  $a = 2.54343m$  there is only one photon sphere at  $r_m = 2.29825m$  and for  $a > 2.54343m$  there are no photon spheres and no horizons.

- for  $n = 1$  and  $k = 2$ , one has two horizons for  $a < \frac{4m}{3\sqrt{3}}$  and two photon spheres for  $a < \frac{2m}{\sqrt{5}}$  while for  $a = \frac{2m}{\sqrt{5}}$  it has one photon sphere at  $r_m = \frac{4m}{\sqrt{5}}$  and for  $a > \frac{2m}{\sqrt{5}}$  it has no photon spheres and no horizons.

If we simply substitute  $r_m$  for  $r_0$  into (8), the integral diverges [49], which is expected because a photon becomes trapped in the photon surface. Thus, the light deflection angle  $\alpha$  is calculated with  $r_0 \rightarrow r_m$  in the strong field limit. When  $r_0 \rightarrow r_m$ , the impact parameter approaches a critical value ( $b_c$ ), so we can also express the deflection angle in terms of  $b_c$  instead of  $r_m$ , which will become more convenient in Section V where we calculate the observables. We can compare graphically how  $b_c$  changes with  $a$  among the black-bounce

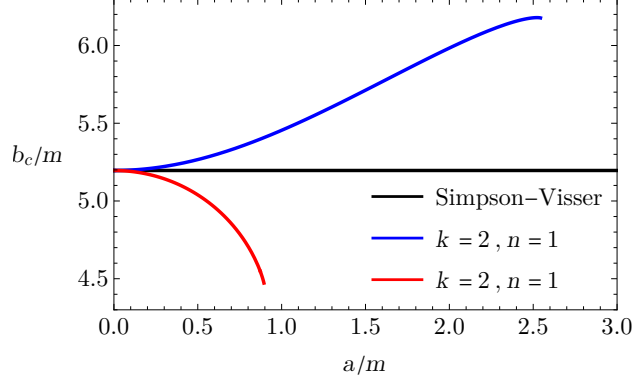


Figure 4: Critical impact parameter as a function of  $a$ .

spacetimes (see Fig. 4): The only black-bounce metric with a closed form of the critical impact parameter is the SV metric, for which  $b_c = 3\sqrt{3}m$ , the same as Schwarzschild, independent of  $a$ . For the other two black-bounce metrics,  $b_c$  depends on the value of  $a$ .

Since the integral diverges in this case, the method devised in [49] can be used to extract the divergent part of the result. It remains to evaluate the regular part of the integral. The result looks like:

$$\alpha(b) \approx -\mathcal{A} \ln \left( \frac{b}{b_c} - 1 \right) + \mathcal{B}, \quad (12)$$

where the coefficients  $\mathcal{A}$  and  $\mathcal{B}$  are constants, and the logarithmic term diverges in the strong field limit ( $b \rightarrow b_c$ ). The constant  $\mathcal{A}$  is given by:

$$\mathcal{A} = \frac{1}{\sqrt{f_m - \frac{1}{2}f_m''\Sigma_m^2}}. \quad (13)$$

And the constant  $\mathcal{B}$  looks like:

$$\mathcal{B} = \mathcal{A} \ln \left( r_m^2 \left( \frac{2}{\Sigma_m^2} - \frac{f_m''}{f_m} \right) \right) + I_R - \pi. \quad (14)$$

In this expression,  $I_R$  is the regular part (15) of the integral of the light deflection (*cf.* (8)):

$$I_R = \int_0^1 dz \left( \frac{2r_m}{(1-z)^2 \sqrt{\frac{f_m}{\Sigma_m^2} \Sigma^4\left(\frac{r_m}{1-z}\right) - \Sigma^2\left(\frac{r_m}{1-z}\right) f\left(\frac{r_m}{1-z}\right)}} - \frac{2}{z \sqrt{f_m - \frac{1}{2}f_m''\Sigma_m^2}} \right) \quad (15)$$

where  $z = 1 - \frac{r_0}{r}$  as defined in [49]. The first term inside the integral is just the integrand of (8) after substituting  $z$  for  $r$  and  $r_m$  for  $r_0$ . The second term inside the integral is the divergent term, which is used to calculate the strong field coefficients  $\mathcal{A}$  and  $\mathcal{B}$ , so we subtract the divergent term from the original integral to obtain a finite result and the divergent part

becomes a logarithmic function which tends to infinity. For the metric with  $k = 0, n = 2$ , this expression becomes

$$\int_0^1 \frac{2r_m dz}{\sqrt{(r_m^2 + a^2(z-1)^2) \left( \frac{(r_m^2 + a^2(z-1)^2)(\sqrt[4]{r_m^4 + a^4} - 2m)}{(r_m^2 + a^2)\sqrt[4]{r_m^4 + a^4}} - \frac{2m(z-1)^3}{\sqrt[4]{r_m^4 + a^4}(z-1)^4} - (z-1)^2 \right)}} - \int_0^1 \frac{2(r_m^4 + a^4)^{\frac{9}{8}} dz}{z \sqrt{2a^2 m r_m^6 - 7a^4 m r_m^4 - 3a^6 m r_m^2 - 2a^8 m + (r_m^4 + a^4)^{\frac{9}{4}}}}, \quad (16)$$

where, as a result of Eq.(10),  $r_m$  is given by the following equation

$$(a^4 + r_m^4)^{5/4} - m(2a^4 + a^2 r_m^2 + 3r_m^4) = 0. \quad (17)$$

And for  $k = 2, n = 1$  the regular integral is written as

$$\int_0^1 \frac{2r_m dz}{\sqrt{\frac{(r_m^2 + a^2(z-1)^2)((r_m^2 + a^2)^{\frac{3}{2}} - 2mr_m^2)}{(r_m^2 + a^2)^{\frac{5}{2}}} - r_m^2(z-1)^2 \left( 1 + \frac{2m(z-1)}{\sqrt{r_m^2 + a^2}(z-1)^2} \right) - a^2(z-1)^4}} - \int_0^1 \frac{2(r_m^2 + a^2)^{\frac{5}{4}} dz}{z \sqrt{ma^2(2a^2 - 13rm^2) + (r_m^2 + a^2)^{\frac{5}{2}}}}, \quad (18)$$

where, as a result of Eq.(10),  $r_m$  satisfies the following equation

$$a^2 \left( \sqrt{a^2 + r_m^2} + 2m \right) + r_m^2 \left( \sqrt{a^2 + r_m^2} - 3m \right) = 0. \quad (19)$$

In Fig. 5 we compare the results of the regular integral for the metrics whose photon spheres were previously illustrated with the regular integral for the SV metric. We can see in this figure that as  $a$  approaches a limit for which there can no longer be photon spheres, the regular integral diverges, tending to  $+\infty$  for SV space-time and to  $-\infty$  for the generalized black-bounce space-times. For small values of  $a$ , the regular integral does not depend on  $n$  and  $k$ .

As illustrated in Fig. 6, when we increase  $a$ , not only the curves become different, but the critical impact parameters and the value for which the deflection angle blows up, present differences. As we restricted ourselves here to the strong field limit, we did not calculate the deflection for values of  $a$  for which the metric does not exhibit photon spheres. This is the reason why there is no  $k = 2$  curve for  $a = \frac{5}{2}m$  (its limit for photon spheres is  $a = \frac{2m}{\sqrt{5}}$ ).

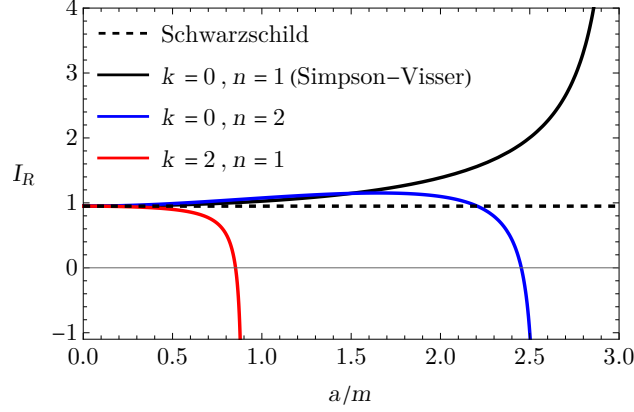


Figure 5: Regular integral as a function of parameter  $a$ .

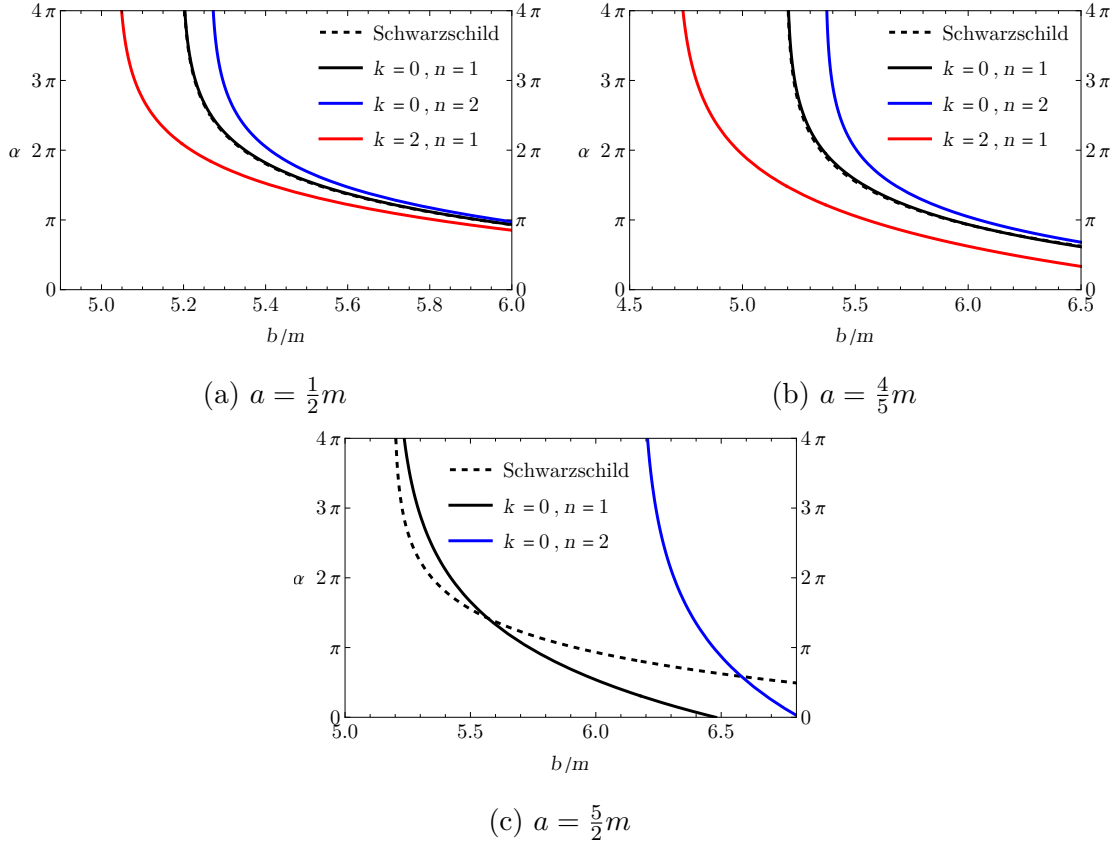


Figure 6: Strong field approximation for different space-times and fixed  $a$ .

## V. GRAVITATIONAL LENSING

After we have written light deflection in the form of (12), it becomes possible to calculate two physical quantities related to the nearest surroundings of a black hole outside its shadow. In the strong field limit, relativistic images are located very close to the main image. They are

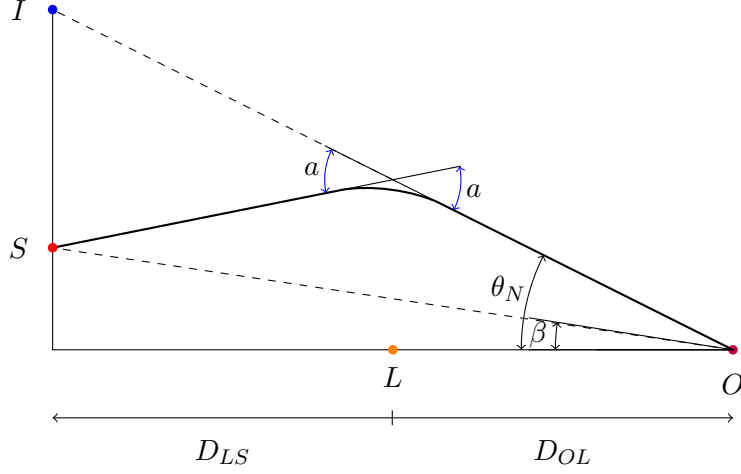


Figure 7: Schematic representation of the observer (O), the source (S), the lens (L) and the image (I).

formed by photons from some source behind the black hole whose impact parameter results in a deflection of more than  $2\pi$ , i.e. they do more than one turn around the black hole before coming out to the observer. Relativistic images are also fainter and more compact than the main image. There is a relativistic image for each number ( $N$ ) of complete rotations. We follow the same procedure adopted in [49, 67, 71, 72].

### A. Lens equation

Let us exclude all full rotations by defining  $\alpha_N \equiv \alpha - 2\pi N$ . Then we can calculate the difference between the angular positions of the source ( $\beta$ ) and of the image seen by observers ( $\theta_N$ ), illustrated in Fig. 7. The relation between these angles is the Lens Equation (20).

$$\beta = \theta_N - \frac{D_{LS}}{D_{OS}} \alpha_N. \quad (20)$$

Here we suppose  $D_{OS} \approx D_{LS} + D_{OL}$ , for the angle  $\alpha_N$  must be tiny to guarantee the visibility for lensing effects. In this regard, it follows from geometrical reasons that  $b \approx D_{OL} \tan \theta_N \approx D_{OL} \theta_N$ .

Thus,  $\alpha_N$  can be treated as a function of  $\theta_N$ . Then, we expand  $\beta$  to first order in  $(\theta_N - \theta_N^0)$ , with  $\theta_N^0$  defined as an angle such that  $\alpha_N(\theta_N^0) = 0$ .

$$\beta \approx \theta_N^0 + \left( 1 + \frac{\mathcal{A} D_{LS} D_{OL}}{b_c D_{OS}} e^{\frac{2\pi N - \mathcal{B}}{\mathcal{A}}} \right) (\theta_N - \theta_N^0) \quad (21)$$

This expression can also be easily inverted in order to obtain the angular position of the image ( $\theta_N$ ) as a function of the angular position of the source ( $\beta$ ), by noting that in (21) one can neglect 1 in comparison with another term. So, one finds

$$\theta_N \approx \theta_N^0 + \frac{b_c D_{OS}}{\mathcal{A} D_{OL} D_{LS}} e^{\frac{\mathcal{B}-2\pi N}{\mathcal{A}}} (\beta - \theta_N^0). \quad (22)$$

From (21) and (22) we can define the observables which depend on the deflection coefficients  $\mathcal{A}$  and  $\mathcal{B}$ .

## B. Observables

The first observable is the separation angle ( $s$ ) between the first ( $N = 1$ ) and the remaining relativistic images, all merged in a single image denoted by an infinity index ( $N \rightarrow \infty$ ). Since the correction in (22) is much smaller than  $\theta_N^0$ ,  $s$  can be approximated as follows:

$$s \approx \theta_1^0 - \theta_\infty^0 = \frac{b_c}{D_{OL}} e^{\frac{\mathcal{B}-2\pi}{\mathcal{A}}}. \quad (23)$$

The other observable defined from the deflection coefficients is the ratio between the luminous flux of the first relativistic image and the remaining ones. It depends on the magnification  $\mu_N \equiv \left( \frac{\beta}{\theta_N} \frac{\partial \beta}{\partial \theta_N} \right)^{-1} \Big|_{\theta_N^0}$ . Because of the large distances involved the magnification can be approximated as

$$\mu_N = \frac{b_c^2 D_{OS} e^{\frac{\mathcal{B}-2\pi N}{\mathcal{A}}} \left( 1 + e^{\frac{\mathcal{B}-2\pi N}{\mathcal{A}}} \right)}{\beta \mathcal{A} D_{LS} D_{OL}^2}. \quad (24)$$

Hence, we calculate  $R$ , and, from the order of magnitude of the quantities considered, present its approximate value as:

$$R \equiv \frac{\mu_1}{\sum_2^\infty \mu_N} = \left( e^{\frac{2\pi}{\mathcal{A}}} + e^{\frac{\mathcal{A}}{\mathcal{B}}} \right) \left( \frac{e^{\frac{2\pi}{\mathcal{A}}}}{e^{\frac{2\pi}{\mathcal{A}}} - 1} + \frac{e^{\frac{\mathcal{A}}{\mathcal{B}}}}{e^{\frac{4\pi}{\mathcal{A}}} - 1} \right) \approx e^{\frac{2\pi}{\mathcal{A}}}. \quad (25)$$

## C. Application for *Sagittarius A\**

In order to compare the results of each metric, we suppose the lens is the black hole at the center of the galaxy, *Sagittarius A\**, with mass ( $4.297 \times 10^6 M_\odot$ ) and distance (8277 pc) profile taken from [73]. Fig. 8 presents the separation angles and ratios between luminosities for the metrics studied. We can see in the graphs that the observables can differ essentially from the Schwarzschild case, if the values of  $a$  are not too small.

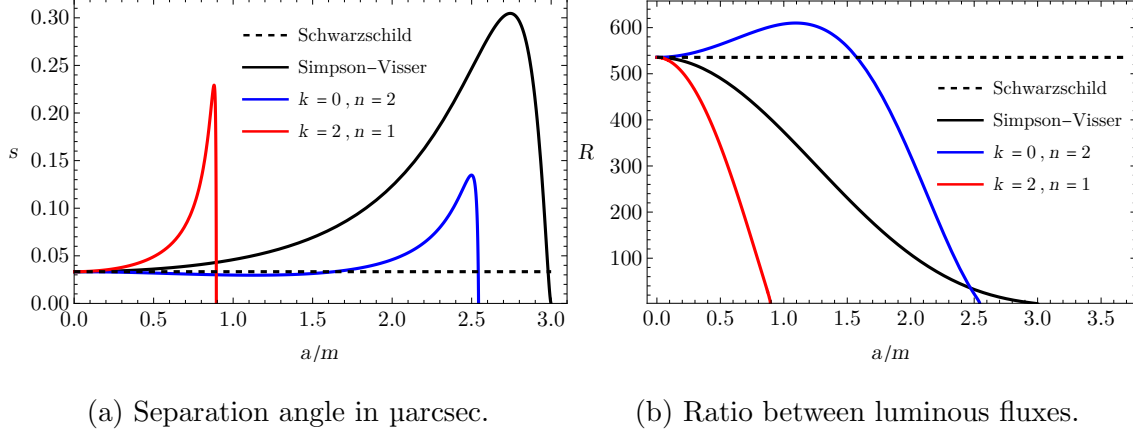


Figure 8: Observables as a function of parameter  $a$  with *Sagittarius* A\* acting as a gravitational lens.

#### D. Shadows

Black hole and wormhole shadows are typical gravitational lensing effects that arise in the strong field regime. As discussed in the previous section, the photon sphere – with critical radius  $r_m$  – is the region where photons are forced to follow unstable circular orbits. As a result, such orbits cast a dark region on the observer’s sky, called the shadow. In particular, for a static and spherically symmetric metric, the radius of the shadow regarding an observer at infinity can be expressed as

$$r_s = \frac{r_m}{\sqrt{f(r_m)}}. \quad (26)$$

For the special case of the SV metric, which corresponds to

$$r_m = 3\sqrt{m^2 - \left(\frac{a}{3}\right)^2} \quad \text{and} \quad f(r_m) = \frac{1}{3}, \quad (27)$$

one can find an analytical expression for the radius of the shadow given by

$$r_s = 3\sqrt{3}\sqrt{m^2 - \left(\frac{a}{3}\right)^2}, \quad (28)$$

which recovers the standard result (Schwarzschild black hole) for  $a = 0$ . From the previous equation, it is straightforward that while  $a$  grows,  $r_s$  decreases – with an upper bound on the bounce parameter given by  $a = 3m$ . Note, however, that depending on the value of  $a$ , the spacetime can represent either a black hole or a wormhole. As discussed in Sec. IV, black holes are recovered for  $0 < a \leq 2m$ , and wormholes with nontrivial photon spheres are obtained for  $2m < a \leq 3m$ .

To further illustrate these cases, we explore how the size of the shadows is affected by the bounce parameter  $a$ . In Fig. 9, we plot shadow size for the SV metric for different values of  $a$ , assuming  $m = 1$ . The reference (dashed) line represents the Schwarzschild photon sphere, while the disk  $a = 0$  describes the size of the Schwarzschild black hole shadow. The other curves,  $a = 1.5$  and  $a = 2.5$ , describe an SV black hole and an SV wormhole, respectively.

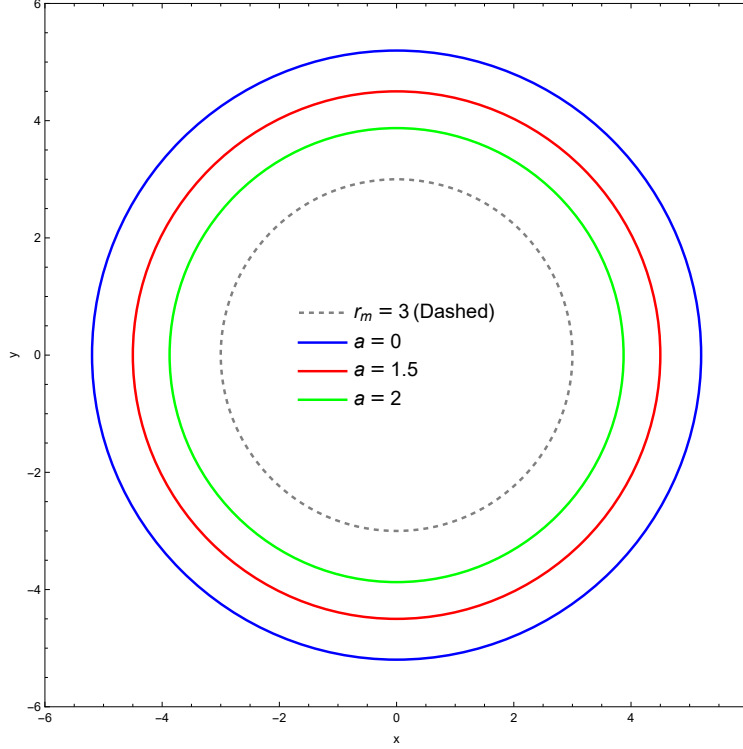


Figure 9: The circles represent the shadow disks for the SV metric for different values of  $a$  for fixed  $m = 1$ . In particular, the outermost circle, blue line ( $a = 0$ ), is the Schwarzschild shadow disk. The dashed circle stands for the Schwarzschild photon sphere.

Now, we turn our attention to generalized black-bounce metrics. We illustrate the size of the shadows for  $k = 2$  and  $n = 1$ , and  $k = 0$  and  $n = 2$  generalized black-bounce metrics. For the former case ( $k = 2$  and  $n = 1$ ), Fig.10 exhibits a global behavior similar to that of the SV metric. Schwarzschild black hole corresponds to the largest shadow disk (blue line in Fig. 10). Notably, the curves,  $a = 0.5$  and  $a = 0.7$ , describe the shadow disks of black holes, while  $a = 0.8$  represents a shadow disk of a wormhole. Fig. 11 displays the behavior of the shadow disks for the case,  $k = 0$  and  $n = 2$ . The qualitative results are similar to those of the two previous cases, as can be seen in Fig.11. Again, the outermost shadow disk corresponds to the Schwarzschild black hole. Note that the curves,  $a = 1$  and  $a = 1.57532$ ,



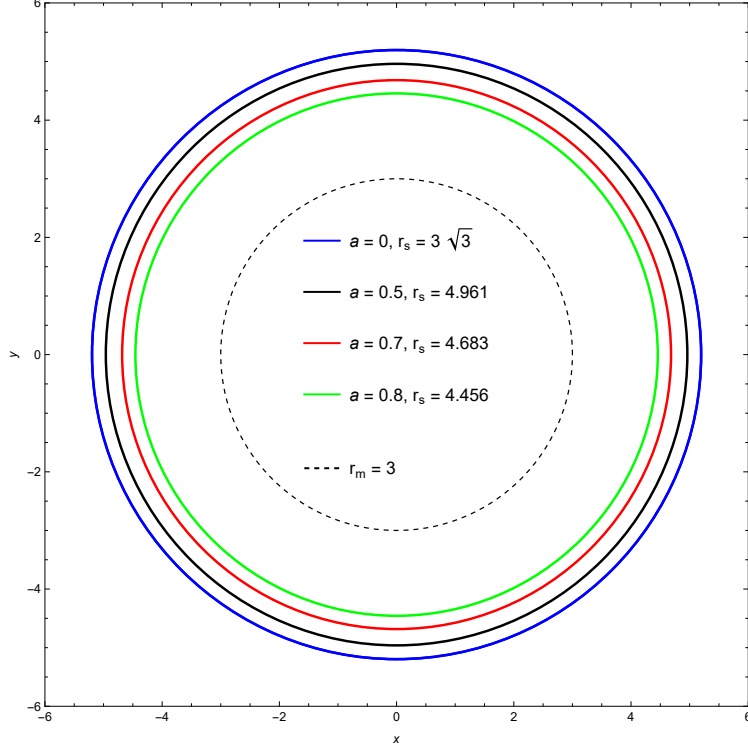


Figure 10: The circles represent the shadow disks for the generalized black-bounce metric ( $k = 2$  and  $n = 1$ ) for different values of  $a$  for fixed  $m = 1$ . Similar to the previous case, the outermost circle, blue line ( $a = 0$ ), represents the Schwarzschild shadow disk, while the dashed one stands for the Schwarzschild photon sphere.

correspond to black holes, whereas the curve  $a = 2.3$  describes a wormhole.

Hence, our results show that, at least for the generalized black-bounce metrics considered, the Schwarzschild black hole exhibits the largest shadow. This is not surprising, because this topic has been explored in the literature for other kinds of static and spherically symmetric spacetimes [74]. In fact, the authors of [74] postulated a sequence of inequalities for the parameters characterizing the size of the black hole, i.e.,

$$\frac{3}{2}r_{sc} \leq r_m \leq \frac{r_s}{\sqrt{3}} \leq 3m, \quad (29)$$

where  $r_{sc} = 2m$ . Note that the generalized black-bounce metrics considered here do not satisfy the above inequalities since, as displayed in Fig. 3b, the radius of the photon sphere,  $r_m$ , for  $k = 0$  and  $n = 2$  metric may be bigger than  $3m$ . Although the Schwarzschild black hole remains with the largest shadow size.

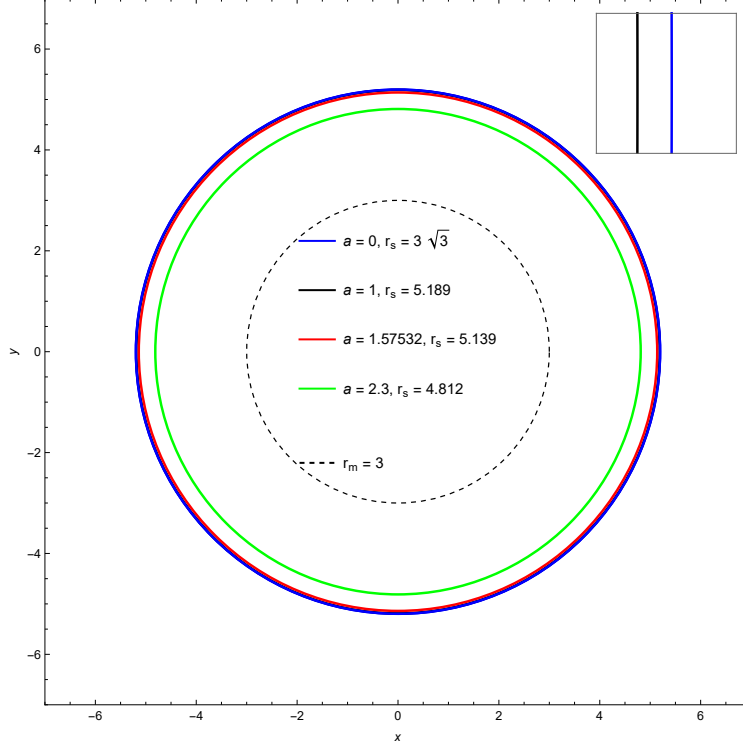


Figure 11: The circles represent the shadow disks for the generalized black-bounce metric ( $k = 0$  and  $n = 2$ ) for different values of  $a$  for fixed  $m = 1$ . The inset figure shows the narrow area between the outermost (blue) circle (Schwarzschild shadow disk) and the black circle ( $a = 1$  and  $r_s = 5.189 < 3\sqrt{3}$ ).

## VI. CONCLUSIONS

In this work, we have analyzed light deflection and gravitational lensing in  $k - n$  generalized black-bounce spacetimes, characterized by two parameters,  $k$  and  $n$ . In the weak-field gravitational regime, we succeeded in demonstrating that the angular deflection within generalized black-bounce metrics coincides with the usual SV metric up to the second order in the parameters,  $a$  and  $m$ . Conversely, in the strong-field regime the critical impact parameter and the bending angle acquire nonlinear dependence on the bounce parameter  $a$  for the cases  $(k = 0, n = 2)$  and  $(k = 2, n = 1)$ , leaving light-bending effects more evident as  $a$  grows. Using the lens equations for *Sagittarius A\**, we demonstrated how relativistic image observables depart from their Schwarzschild values as  $a/m$  increases. Finally, by computing the shadow radii for several black-bounce models, we confirmed that the Schwarzschild black hole produces the largest shadow size.

As an unfolding of this work, we intended to study the light deflection for spinning generalized black-bounce metrics and the rotation effects on their shadows. We plan to carry out these investigations in a forthcoming paper.

**Acknowledgments.** This work was partially supported by Conselho Nacional de Desenvolvimento Científico e Tecnológico (CNPq). The work by A. Yu. P. has been partially supported by the CNPq project No. 303777/2023-0. The work by P. J. P. has been partially supported by the CNPq project No. 307628/2022-1.

- 
- [1] F. W. Dyson, A. S. Eddington, and C. Davidson, “A Determination of the Deflection of Light by the Sun’s Gravitational Field, from Observations Made at the Total Eclipse of May 29, 1919,” *Phil. Trans. Roy. Soc. Lond. A*, vol. 220, pp. 291–333, 1920.
  - [2] L. C. B. Crispino and S. Paolantonio, “The first attempts to measure light deflection by the Sun,” *Nature Astron.*, vol. 4, p. 6, 2020.
  - [3] J. A. S. Lima and R. C. Santos, “Do Eclipse Solar de 1919 ao Espetáculo das Lentes Gravitacionais,” *Revista Brasileira de Ensino de Física*, vol. 41, p. e20190199, 2019.
  - [4] K. Akiyama *et al.*, “First M87 Event Horizon Telescope Results. I. The Shadow of the Supermassive Black Hole,” *Astrophys. J. Lett.*, vol. 875, p. L1, 2019.
  - [5] K. Akiyama *et al.*, “First M87 Event Horizon Telescope Results. II. Array and Instrumentation,” *Astrophys. J. Lett.*, vol. 875, no. 1, p. L2, 2019.
  - [6] K. Akiyama *et al.*, “First M87 Event Horizon Telescope Results. III. Data Processing and Calibration,” *Astrophys. J. Lett.*, vol. 875, no. 1, p. L3, 2019.
  - [7] K. Akiyama *et al.*, “First M87 Event Horizon Telescope Results. IV. Imaging the Central Supermassive Black Hole,” *Astrophys. J. Lett.*, vol. 875, no. 1, p. L4, 2019.
  - [8] K. Akiyama *et al.*, “First M87 Event Horizon Telescope Results. V. Physical Origin of the Asymmetric Ring,” *Astrophys. J. Lett.*, vol. 875, no. 1, p. L5, 2019.
  - [9] K. Akiyama *et al.*, “First M87 Event Horizon Telescope Results. VI. The Shadow and Mass of the Central Black Hole,” *Astrophys. J. Lett.*, vol. 875, no. 1, p. L6, 2019.
  - [10] S. Vagnozzi *et al.*, “Horizon-scale tests of gravity theories and fundamental physics from the Event Horizon Telescope image of Sagittarius A,” *Class. Quant. Grav.*, vol. 40, no. 16, p. 165007, 2023.

- [11] A. Einstein, “Lens-Like Action of a Star by the Deviation of Light in the Gravitational Field,” *Science*, vol. 84, pp. 506–507, 1936.
- [12] S. Liebes, “Gravitational Lenses,” *Phys. Rev.*, vol. 133, pp. B835–B844, 1964.
- [13] S. Refsdal, “The gravitational lens effect,” *Mon. Not. Roy. Astron. Soc.*, vol. 128, p. 295, 1964.
- [14] A. R. Soares, C. F. S. Pereira, R. L. L. Vitória, M. V. d. S. Silva, and H. Belich, “Light deflection and gravitational lensing effects inspired by loop quantum gravity,” 3 2025.
- [15] J. Kumar, S. U. Islam, and S. G. Ghosh, “Strong gravitational lensing by loop quantum gravity motivated rotating black holes and EHT observations,” *Eur. Phys. J. C*, vol. 83, no. 11, p. 1014, 2023.
- [16] N. Heidari, A. A. Araújo Filho, R. C. Pantig, and A. Övgün, “Absorption, scattering, geodesics, shadows and lensing phenomena of black holes in effective quantum gravity,” *Phys. Dark Univ.*, vol. 47, p. 101815, 2025.
- [17] A. A. A. Filho, J. R. Nascimento, A. Y. Petrov, P. J. Porfírio, and A. Övgün, “Effects of non-commutative geometry on black hole properties,” *Phys. Dark Univ.*, vol. 46, p. 101630, 2024.
- [18] A. A. A. Filho, J. R. Nascimento, A. Y. Petrov, and P. J. Porfírio, “Gravitational lensing by a Lorentz-violating black hole,” 4 2024.
- [19] A. A. Araújo Filho, N. Heidari, and A. Övgün, “Geodesics, accretion disk, gravitational lensing, time delay, and effects on neutrinos induced by a non-commutative black hole,” 12 2024.
- [20] E. F. Eiroa, G. E. Romero, and D. F. Torres, “Reissner-Nordstrom black hole lensing,” *Phys. Rev. D*, vol. 66, p. 024010, 2002.
- [21] E. F. Eiroa and D. F. Torres, “Strong field limit analysis of gravitational retro lensing,” *Phys. Rev. D*, vol. 69, p. 063004, 2004.
- [22] N. Tsukamoto and Y. Gong, “Retrolensing by a charged black hole,” *Phys. Rev. D*, vol. 95, no. 6, p. 064034, 2017.
- [23] L. Chetouani and G. Clément, “Geometrical optics in the ellis geometry,” *General relativity and gravitation*, vol. 16, pp. 111–119, 1984.
- [24] V. Perlick, “On the Exact gravitational lens equation in spherically symmetric and static space-times,” *Phys. Rev. D*, vol. 69, p. 064017, 2004.
- [25] K. K. Nandi, Y.-Z. Zhang, and A. V. Zakharov, “Gravitational lensing by wormholes,” *Phys.*

- Rev. D*, vol. 74, p. 024020, 2006.
- [26] T. K. Dey and S. Sen, “Gravitational lensing by wormholes,” *Mod. Phys. Lett. A*, vol. 23, pp. 953–962, 2008.
  - [27] A. Bhattacharya and A. A. Potapov, “Bending of light in Ellis wormhole geometry,” *Mod. Phys. Lett. A*, vol. 25, pp. 2399–2409, 2010.
  - [28] K. Nakajima and H. Asada, “Deflection angle of light in an Ellis wormhole geometry,” *Phys. Rev. D*, vol. 85, p. 107501, 2012.
  - [29] N. Tsukamoto, T. Harada, and K. Yajima, “Can we distinguish between black holes and wormholes by their Einstein ring systems?,” *Phys. Rev. D*, vol. 86, p. 104062, 2012.
  - [30] K. K. Nandi, A. A. Potapov, R. N. Izmailov, A. Tamang, and J. C. Evans, “Stability and instability of Ellis and phantom wormholes: Are there ghosts?,” *Phys. Rev. D*, vol. 93, no. 10, p. 104044, 2016.
  - [31] N. Tsukamoto, “Strong deflection limit analysis and gravitational lensing of an Ellis wormhole,” *Phys. Rev. D*, vol. 94, no. 12, p. 124001, 2016.
  - [32] N. Tsukamoto, “Retrolensing by a wormhole at deflection angles  $\pi$  and  $3\pi$ ,” *Phys. Rev. D*, vol. 95, no. 8, p. 084021, 2017.
  - [33] N. Tsukamoto and T. Harada, “Light curves of light rays passing through a wormhole,” *Phys. Rev. D*, vol. 95, no. 2, p. 024030, 2017.
  - [34] R. Shaikh, P. Banerjee, S. Paul, and T. Sarkar, “A novel gravitational lensing feature by wormholes,” *Phys. Lett. B*, vol. 789, pp. 270–275, 2019. [Erratum: *Phys.Lett.B* 791, 422–423 (2019)].
  - [35] R. Shaikh, P. Banerjee, S. Paul, and T. Sarkar, “Strong gravitational lensing by wormholes,” *JCAP*, vol. 07, p. 028, 2019. [Erratum: *JCAP* 12, E01 (2023)].
  - [36] H. Aounallah, A. R. Soares, and R. L. L. Vitória, “Scalar field and deflection of light under the effects of topologically charged Ellis–Bronnikov-type wormhole spacetime,” *Eur. Phys. J. C*, vol. 80, no. 5, p. 447, 2020.
  - [37] A. B. Aazami, C. R. Keeton, and A. O. Petters, “Lensing by Kerr Black Holes. I: General Lens Equation and Magnification Formula,” *J. Math. Phys.*, vol. 52, p. 092502, 2011.
  - [38] A. B. Aazami, C. R. Keeton, and A. O. Petters, “Lensing by Kerr Black Holes. II: Analytical Study of Quasi-Equatorial Lensing Observables,” *J. Math. Phys.*, vol. 52, p. 102501, 2011.
  - [39] V. Bozza and G. Scarpetta, “Strong deflection limit of black hole gravitational lensing with

- arbitrary source distances,” *Phys. Rev. D*, vol. 76, p. 083008, 2007.
- [40] V. Bozza, F. De Luca, G. Scarpetta, and M. Sereno, “Analytic Kerr black hole lensing for equatorial observers in the strong deflection limit,” *Phys. Rev. D*, vol. 72, p. 083003, 2005.
  - [41] V. Bozza, F. De Luca, and G. Scarpetta, “Kerr black hole lensing for generic observers in the strong deflection limit,” *Phys. Rev. D*, vol. 74, p. 063001, 2006.
  - [42] V. Bozza, “Quasiequatorial gravitational lensing by spinning black holes in the strong field limit,” *Phys. Rev. D*, vol. 67, p. 103006, 2003.
  - [43] S. Chen, S. Wang, Y. Huang, J. Jing, and S. Wang, “Strong gravitational lensing for the photons coupled to a Weyl tensor in a Kerr black hole spacetime,” *Phys. Rev. D*, vol. 95, no. 10, p. 104017, 2017.
  - [44] K. S. Virbhadra and G. F. R. Ellis, “Schwarzschild black hole lensing,” *Phys. Rev. D*, vol. 62, p. 084003, 2000.
  - [45] C.-M. Claudel, K. S. Virbhadra, and G. F. R. Ellis, “The Geometry of photon surfaces,” *J. Math. Phys.*, vol. 42, pp. 818–838, 2001.
  - [46] S. Frittelli, T. P. Kling, and E. T. Newman, “Space-time perspective of Schwarzschild lensing,” *Phys. Rev. D*, vol. 61, p. 064021, 2000.
  - [47] V. Bozza, S. Capozziello, G. Iovane, and G. Scarpetta, “Strong field limit of black hole gravitational lensing,” *Gen. Rel. Grav.*, vol. 33, pp. 1535–1548, 2001.
  - [48] V. Bozza, “Gravitational lensing in the strong field limit,” *Phys. Rev. D*, vol. 66, p. 103001, 2002.
  - [49] N. Tsukamoto, “Deflection angle in the strong deflection limit in a general asymptotically flat, static, spherically symmetric spacetime,” *Phys. Rev. D*, vol. 95, p. 064035, Mar. 2017. <https://doi.org/10.1103/PhysRevD.95.064035>.
  - [50] F. Feleppa, V. Bozza, and O. Y. Tsupko, “Strong deflection limit analysis of black hole lensing in inhomogeneous plasma,” *Phys. Rev. D*, vol. 110, no. 6, p. 064031, 2024.
  - [51] F. Feleppa, V. Bozza, and O. Y. Tsupko, “Strong deflection of massive particles in spherically symmetric spacetimes,” *Phys. Rev. D*, vol. 111, no. 4, p. 044018, 2025.
  - [52] C. Furtado, J. R. Nascimento, A. Y. Petrov, P. J. Porfírio, and A. R. Soares, “Strong gravitational lensing in a spacetime with topological charge within the Eddington-inspired Born-Infeld gravity,” *Phys. Rev. D*, vol. 103, no. 4, p. 044047, 2021.
  - [53] N. Tsukamoto, “Gravitational lensing by using the 0th order of affine perturbation series of

- the deflection angle of a ray near a photon sphere,” *Eur. Phys. J. C*, vol. 83, no. 4, p. 284, 2023.
- [54] A. R. Soares, R. L. L. Vitória, and C. F. S. Pereira, “Topologically charged holonomy corrected Schwarzschild black hole lensing,” *Phys. Rev. D*, vol. 110, no. 8, p. 084004, 2024.
  - [55] K. S. Virbhadra, “Conservation of distortion of gravitationally lensed images,” *Phys. Rev. D*, vol. 109, no. 12, p. 124004, 2024.
  - [56] K. S. Virbhadra, “Compactness of supermassive dark objects at galactic centers,” *Can. J. Phys.*, vol. 102, p. 512, 2024.
  - [57] J. Bardeen, “Non-singular general relativistic gravitational collapse,” in *Proceedings of the 5th International Conference on Gravitation and the Theory of Relativity*, p. 87, Sept. 1968.
  - [58] A. Bogojevic and D. Stojkovic, “A Nonsingular black hole,” *Phys. Rev. D*, vol. 61, p. 084011, 2000.
  - [59] S. A. Hayward, “Formation and evaporation of regular black holes,” *Phys. Rev. Lett.*, vol. 96, p. 031103, 2006.
  - [60] C. Bambi and L. Modesto, “Rotating regular black holes,” *Phys. Lett. B*, vol. 721, pp. 329–334, 2013.
  - [61] B. Toshmatov, B. Ahmedov, A. Abdujabbarov, and Z. Stuchlik, “Rotating Regular Black Hole Solution,” *Phys. Rev. D*, vol. 89, no. 10, p. 104017, 2014.
  - [62] M. Azreg-Aïnou, “Generating rotating regular black hole solutions without complexification,” *Phys. Rev. D*, vol. 90, no. 6, p. 064041, 2014.
  - [63] E. Ayon-Beato and A. Garcia, “Regular black hole in general relativity coupled to nonlinear electrodynamics,” *Phys. Rev. Lett.*, vol. 80, pp. 5056–5059, 1998.
  - [64] A. Simpson and M. Visser, “Black-bounce to traversable wormhole,” *JCAP*, vol. 02, p. 042, 2019.
  - [65] A. Simpson, P. Martin-Moruno, and M. Visser, “Vaidya spacetimes, black-bounces, and traversable wormholes,” *Class. Quant. Grav.*, vol. 36, no. 14, p. 145007, 2019.
  - [66] Z.-Y. Fan and X. Wang, “Construction of Regular Black Holes in General Relativity,” *Phys. Rev. D*, vol. 94, no. 12, p. 124027, 2016.
  - [67] J. R. Nascimento, A. Y. Petrov, P. J. Porfirio, and A. R. Soares, “Gravitational lensing in black-bounce spacetimes,” *Phys. Rev. D*, vol. 102, no. 4, p. 044021, 2020.
  - [68] F. S. N. Lobo, M. E. Rodrigues, M. V. d. S. Silva, A. Simpson, and M. Visser, “Novel black-

- bounce spacetimes: Wormholes, regularity, energy conditions, and causal structure,” *Phys. Rev. D*, vol. 103, p. 084052, Apr. 2021. <https://doi.org/10.1103/PhysRevD.103.084052>.
- [69] N. Tsukamoto, “Gravitational lensing in the Simpson-Visser black-bounce spacetime in a strong deflection limit,” *Phys. Rev. D*, vol. 103, p. 024033, Jan. 2021. <https://doi.org/10.1103/PhysRevD.103.024033>.
- [70] K. A. Bronnikov and R. K. Walia, “Field sources for Simpson-Visser spacetimes,” *Phys. Rev. D*, vol. 105, no. 4, p. 044039, 2022.
- [71] V. Bozza, “Gravitational lensing in the strong field limit,” *Phys. Rev. D*, vol. 66, p. 103001, Nov. 2002.
- [72] V. Bozza, S. Capozziello, G. Iovane, and G. Scarpetta, “Strong field limit of black hole gravitational lensing,” *General Relativity and Gravitation*, vol. 33, pp. 1535–1548, 2001.
- [73] GRAVITY Collaboration *et al.*, “Mass distribution in the galactic center based on interferometric astrometry of multiple stellar orbits,” *A&A*, vol. 657, p. L12, Nov. 2022. Table B.1. <https://doi.org/10.1051/0004-6361/202142465>.
- [74] H. Lu and H.-D. Lyu, “Schwarzschild black holes have the largest size,” *Phys. Rev. D*, vol. 101, no. 4, p. 044059, 2020.